Proceedings of the ASME 2016 35th International Conference on Ocean, Offshore and Arctic Engineering
OMAE2016
June 19-24, 2016, Busan, South Korea

OMAE2016-54236

Study of Seabed Trench Induced by Steel Catenary Riser and Seabed Interaction

Kunpeng Wang
Jiangsu University of Science and Technology
Zhenjiang, Jiangsu, China

Ying Min Low
National University of Singapore
Singapore

ABSTRACT

Seabed trench profile has significant effect on the fatigue damage of steel catenary riser near touchdown point. This study briefly demonstrates an approach in literature to determine the seabed trench induced by wave frequency response based on the cubic polynomial model. In this approach, a criterion for the matching between catenary riser and seabed trench is proposed, which is an optimization problem, and needs iterative static analysis of catenary riser. Based on the criterion, the sensitivity of the trench length and position to three parameters is parametrically studied: riser mass per unit length, ratio of horizontal span to vertical span of catenary part, trench depth. The obtained data are employed to fit the equations of trench length and position, which is taken as surrogate model since the iterative static analysis is very complicated. For completeness, the validation against data obtained from hysteretic seabed model is also illustrated. Based on the surrogate model, this study investigates the effect of trench depth on the fatigue damage near touchdown and the effect of the low frequency response on the seabed trench, and some useful conclusions are obtained.

INTRODUCTION

Steel catenary risers (SCRs) are now extensively used in the deep and ultra-deep water oil and gas production due to the features of easy installation, satisfying compatibility with all kinds of floating structures. However, the continuous contact between SCR and seabed makes the touchdown point (TDP) to be one of the critical points prone to fatigue failure, which is a challenging issue in offshore industry. The SCR-seabed interaction can lead to seabed trench development over time. 2H offshore (2002) indicated that conventionally flat seabed model may overestimate the fatigue stress near TDP, while the existence of seabed trench can distribute the stress, thus lead to relative small stress near TDP. Therefore, it is necessary to reasonably take into account the seabed trench during the fatigue damage assessment.

SCR-seabed interaction process is very complicated, and often be modeled using empirically analytical model. Aubeny et al. (2008a, 2009) proposed the seabed plastic deformation model and SCR-seabed interaction model. The latter depicted the SCR-seabed interaction process with the following stages: initial penetration, elastic rebound with full soil-pipe interaction, partial soil-pipe separation, full separation and repenetration. Nakhaee and Zhang (2010) extended the code CABLE3D using the two models, and investigated the seabed trench development and its effect on the stress variation near TDP. Randolph and Quiggin (2009) proposed the nonlinear hysteretic seabed model, and integrated it into commercial software, Orcaflex. This model was in detail verified by using a pipe test in Kaolin (Aubeny et al., 2008b). Elosta et al. (2013, 2014) applied Orcaflex to investigate the effect of the seabed lateral stiffness on the trench development and the fatigue damage near TDP. Shiri (2014a) implemented the nonlinear hysteretic seabed model in ABAQUS based on UEL to study the response of SCR near TDP.

Although above mentioned seabed model can capture the seabed trench development during the SCR global analysis, the process is very slow. The maximum trench depth only achieves 4 to 5 times riser diameters after several months following the SCR installation (Thethi and Moros, 2001). Since the simulation time in the SCR design is limited, a reasonably initial seabed trench may improve the prediction accuracy of fatigue damage near TDP. Bridge and Howells (2003) simply presented the seabed trench profile obtained from the large scale SCR test in STRIDE JIP. Li and Low (2012) and Shiri (2014b) modeled the initial seabed trench using cubic polynomial equation and quadratic exponential equation respectively to study the fatigue damage near TDP. So far there is not a widely accepted seabed trench model in offshore industry, and the research about the effect of the seabed trench on the fatigue damage near TDP often give contradictory conclusions (Shiri, 2014b).

This study briefly introduces an approach proposed by Wang and Low (2015) to calculate the seabed trench induced by wave frequency response, which is termed initial work in the present study. This approach applies cubic polynomial equation to model the trench shape, which needs two additional parameters, trench length and trench position, to well match with SCR. The two parameters are related with lots of factors, such as environmental loads and SCR configuration, but finally taken as functions of riser mass per unit length, the ratio of horizontal span to vertical span of the catenary part and the trench depth. These functions are referred to as surrogate model, and obtained by using the polynomial fitting of the data from iterative static analyses based on the proposed SCR-trench matching criterion. This study applies the surrogate model to investigate the effect of trench depth on the fatigue damage and the effect of the low frequency response on the seabed trench, and some conclusions are obtained.

SEABED MODEL

NONLINEAR HYSTERETIC SEABED MODEL

Nonlinear hysteretic seabed model was integrated into OrcaFlex (Randloph and Quiggin, 2009), and now is widely used in offshore industry. Fig. 1 illustrates the relationship of seabed resistance and penetration described by this model with the following features:

(1) Seabed suction. When the riser uplifts, the seabed resistance would change to suction quickly. The suction would increase from points 2 to 3, and then decrease until SCR-soil separation at point 4.

(2) Seabed trench development. When riser moves downward to point 1 again, it may pierce the trench bottom, thus leads to trench development. It should be noted that the seabed resistance is smaller than the original value when the riser pierce the trench bottom. This in part reflects the seabed plastic deformation.

Table 1 presents the control parameters of the nonlinear hysteretic seabed model and related values used in this study. K_{max} mainly controls the maximum stiffness of the initial penetration curve and the uplift curve; f_{suc} controls the ultimate suction curve; λ_{suc} controls the release speed of the suction and the maximum resistance when reaching the trench bottom; λ_{rep} controls the merging position between the repenetration curve and the uplift curve. Since this model has been widely used in offshore industry, and can well capture the trench development, the initial work took the numerical seabed trench obtained from OrcaFlex as benchmark.

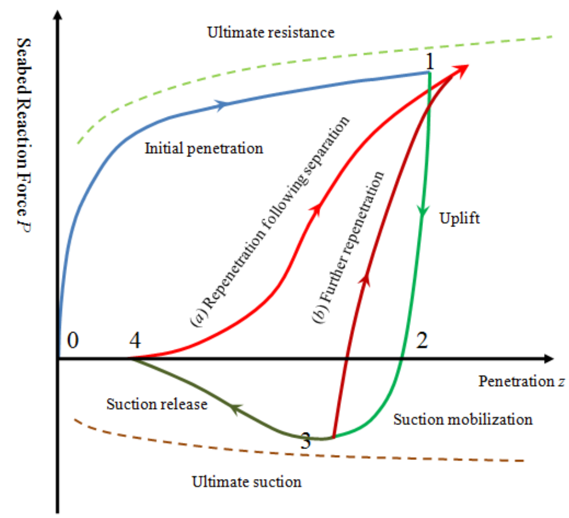

Fig.1 Sketch of nonlinear pipe-soil interaction model

SEABED TRENCH MODEL

Seabed trench development becomes slower and slower with trench depth increasing. Since the simulation time in the numerical analysis is limited, a reasonably initial seabed trench may improve the prediction accuracy of the fatigue damage near TDP. Bridge and Howells (2007) reported the seabed trench in Gulf of Mexico observed using remotely-operation vehicle, and indicated the vertical trench profile is similar with the ladle. Fig. 2 shows the seabed trench sketch. The initial work applied cubic polynomial equation to model trench shape:

$$
\begin{aligned}
d &= d_{\max}\left[c_1\left(\bar{x}/L_T\right)^3 + c_2\left(\bar{x}/L_T\right)^2 + c_3\left(\bar{x}/L_T\right)^1\right] \\
c_1 &= -\left(2\lambda-1\right)/\left[\lambda\left(\lambda-1\right)\right]^2 \\
c_2 &= \left(3\lambda^2-1\right)/\left[\lambda\left(\lambda-1\right)\right]^2 \\
c_3 &= -\left(3\lambda^2-2\lambda\right)/\left[\lambda\left(\lambda-1\right)\right]^2 \\
\lambda &= L_{\max}/L_T
\end{aligned} \tag{1}
$$

where d is the trench depth, $\bar{x}$ is the position relative to TBP, $d_{\max}$ is the maximum penetration depths, $L_{\max}$ is the horizontal length from TBP to TMP, L_T is the trench length. It should be noted that the self-weight penetration in Fig. 2 can be formed during the static analysis, thus is not taken into account in the analytical trench models.

$L_{\max}$ is calculated to be $L_T/3$ by assuming zero slope at TEP, thus L_T becomes the only variable for the two empirical trench models under prescribed $d_{\max}$. Additionally, the relative position of TBP to reference TDP, symbolized as Δ_{TP}, is applied to locate the trench position, see Fig.2.

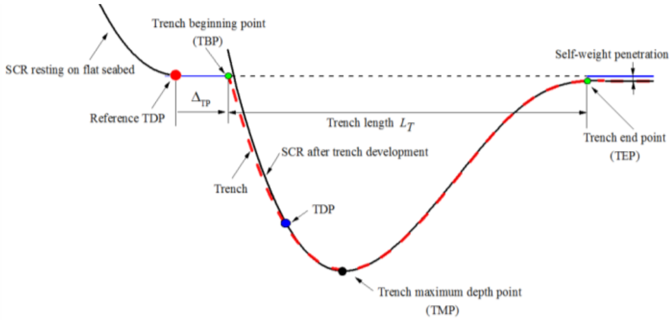

Fig.2 Sketch of seabed trench

ANALYSIS OF SEABED TRENCH

METHODOLOGY

The reasonable length and position of the cubic polynomial trench model are needed to achieve reasonable matching with the static SCR. The initial work took the SCR-trench match as the following optimization problem:

$$\text{Min:}\ \ L_T$$

$$\text{Constraints}\begin{cases} x_{TBP} \le x_{TDP} \le x_{TMP} \\ z_{riser} \le z_{trench} \quad x \in \left[x_{TDP}, x_{TEP}\right] \end{cases} \tag{2}$$

where x and z represent the x- and z- coordinates in global coordinate system.

Fig. 3 is the flowchart of solving the optimization problem, which needs iterative static analysis. The regions A, B and C are defined as follows:

A: L_T and TDP meet the constraint conditions simultaneously.

B: $x_{TDP} < x_{TBP}$ OR Existing $x \in \left[x_{TDP}, x_{TEP}\right]$ meets $z_{riser} > z_{trench}$.

C: $x_{TDP} < x_{TMP}$.

Based on the interface between OrcaFlex and C++, an in-house code was developed to solve the optimization problem. At each iterative analysis, OrcaFlex would be called to carry out static analysis by configuring empirical trench, and then the coordinates of SCR near TDP would be extracted to compare with the trench. According to the coordinate comparison of seabed trench and SCR near TDP, the trench length and position would be updated for the next iterative analysis.

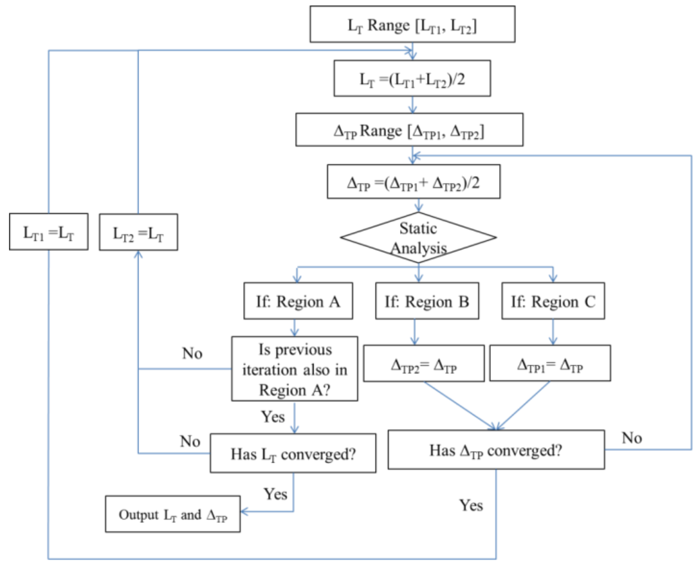

Fig.3 Flowchart for the calculation of the trench length and position

PARAMETRIC ANALYSIS OF TRENCH LENGTH AND POSITION

The initial work assumed that the trench length and position are mainly related with the SCR configuration, mass per unit length and trench depth, and neglected the environment loads, seabed stiffness and riser bending stiffness. For general application, the related parameters are normalized as follows:

$$R_L = \frac{L_T}{D} \qquad R_{TP} = \frac{\Delta_{TP}}{D} \tag{3}$$

$$R_d = \frac{d_{\max}}{D} \qquad R_M = \frac{m}{\rho_f \pi D^2 / 4} \qquad R_{HV} = \frac{H}{V} \tag{4}$$

where D is the riser outer diameter, H and V represent the horizontal and vertical span of the SCR catenary part. R_L and R_{HV} are functions of R_d, R_M and R_{HV}. Table 2 present the value of the normalized parameters, and totally has 504 sets of (R_d, R_M, R_{HV}). A SCR with length of 1610m was applied to carry out the parametric analysis.

Based on the in-house code, the optimum R_L and R_{TP} of all sets (R_d, R_M, R_{HV}) are calculated. For saving space, part results are shown in Figs. 4 and 5, in which the lines represent the results obtained from the surrogate model, i.e. the following equations (5) and (6). R_L increases with increasing R_d and R_{HV}, while deceases with increasing R_M. The sensitivity of R_L to R_M、 R_d and R_{HV} in turn increases. Compared with R_L, R_{TP} is more nonlinear. Negative value of R_{TP} represents that the TBP position of trench moves from the reference TDP position to hang-off point. With trench development, TBP position moves to the hang-off point with decreasing rate of R_{TP} to R_d, see Fig. 5(a). As R_M increases with constant R_d, the TBP position moves toward to the reference TDP position with decreasing rate of R_{TP} to R_M, see Fig. 5(b). When R_{HV} increases, TBP position almost linearly moves toward to hang-off point.

(a)

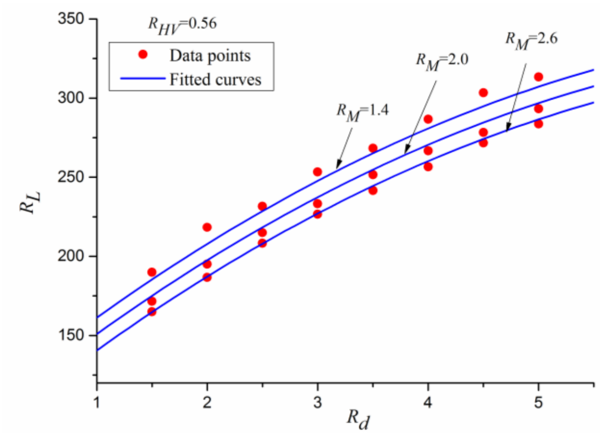

(b)

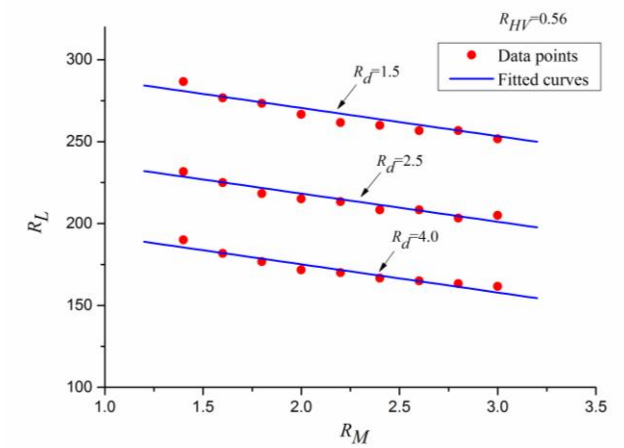

(c)

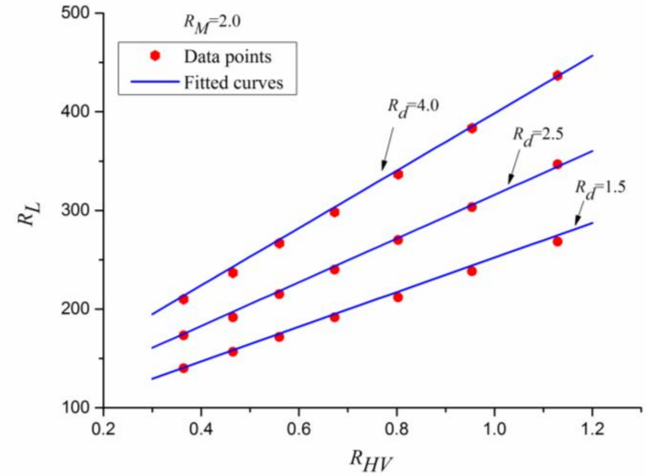

Fig. 4 R_L with different parameters

(a)

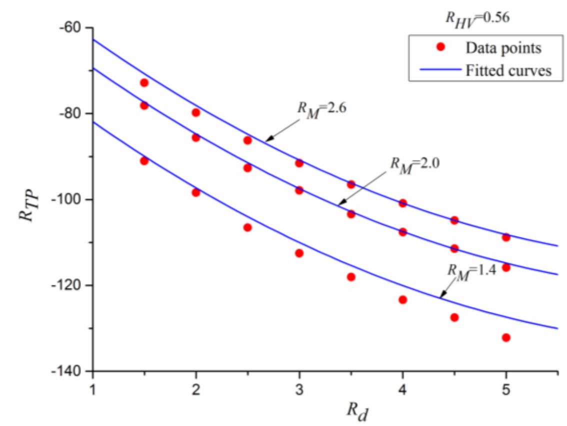

(b)

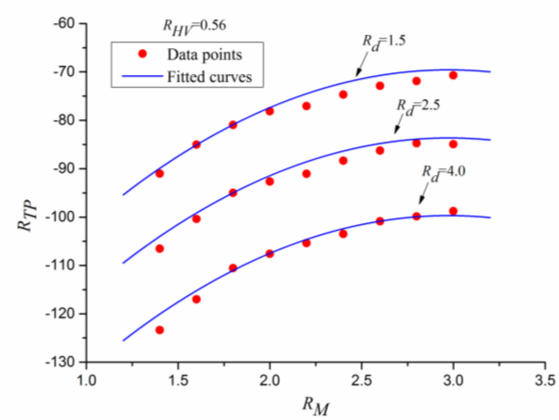

(c)

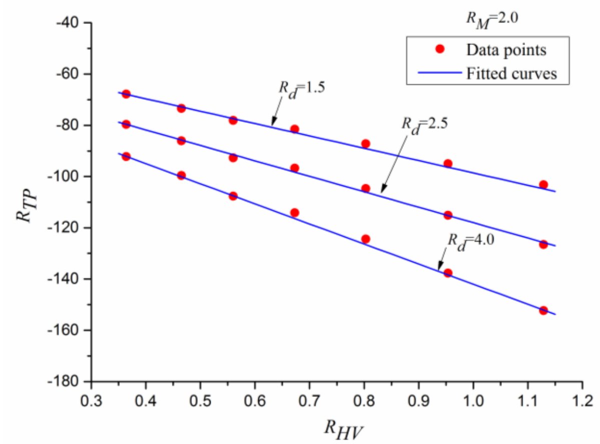

Fig. 5 R_{TP} variation with different parameters

In the initial work, the quadratic polynomial equations were applied to fit the above obtained data. In order to omit the unimportant terms, different combinations of the terms are attempted to find the simplest equations. The simplified fitting equations are given by:

$$R_L = 72.5 + 30.9R_d + 106.1R_{HV} - 17.2R_M - 3.38R_d^2 + 46.2R_d R_{HV} \tag{5}$$

$$R_{TP} = -99.2 - 12.7R_d + 48.8R_M - 30R_{HV} + 13.5R_d^2 - 8.2R_M^2 - 12.1R_d R_{HV} \tag{6}$$

The equations (5) and (6) are taken as surrogate model to replace the iterative static analysis in section 3.1. Coefficient of determination, denoted by R^2, is often used to assess whether a fitting equation well models the data. The closer R^2 approximates to 1.0, the more accurate the fitting equation is. The R^2 values of fitting R_L for full quadratic polynomial equation and equation (5) are 0.998 and 0.995 respectively. As for the fitting of R_{TP}, the values of R^2 for full quadratic polynomial equation and equation (6) are 0.997 and 0.995 respectively.

VALIDATION

The numerical trenches obtained from Orcaflex are applied to validate the surrogate model. Table 3 presents the results. It can be seen that larger R_d and R_{HV} correspond to higher prediction accuracy. The predicted TBP position is closer to the hang-off point than the numerical trench. Overall, the results predicted by surrogate model shows good agreement with the numerical trench.

For further verification, the numerical trench, empirical trench based on iterative static analysis and surrogate model are compared. Fig. 6(*a*) shows the trench profiles with R_d=4.3. The trenches based on the iterative static analysis and surrogate model are almost the same, so the surrogate model can well model the data obtained from iterative static analysis. In addition, the trenches based on iterative static analysis and surrogate model both are a little closer to the hang-off point than the numerical trench, and the related fatigue damages of the SCR near TDP are slightly overestimated, see Fig. 6(*b*).

(a)

(b)

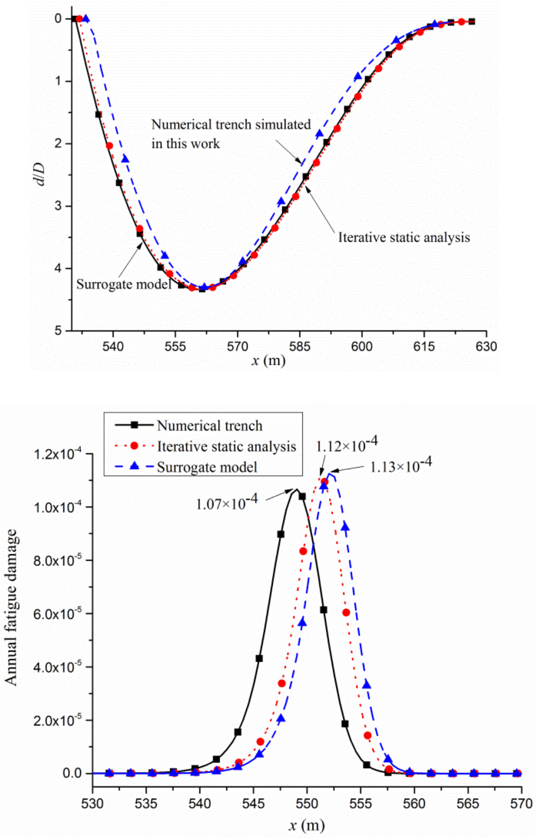

Fig. 6 Empirical seabed trench and related fatigue damage at TDZ

EFFECT OF TRENCH DEPTH ON FATIGUE DAMAGE

Based on the surrogate model, the present study investigates the effect of trench development on the fatigue damage near TDP. Fig. 7 illustrates that larger trench depth corresponds to smaller fatigue damage. Therefore, trench development may benefit the fatigue lift of SCR near TDP. This conclusion coincides with that in Nakhaee and Zhang (2010).

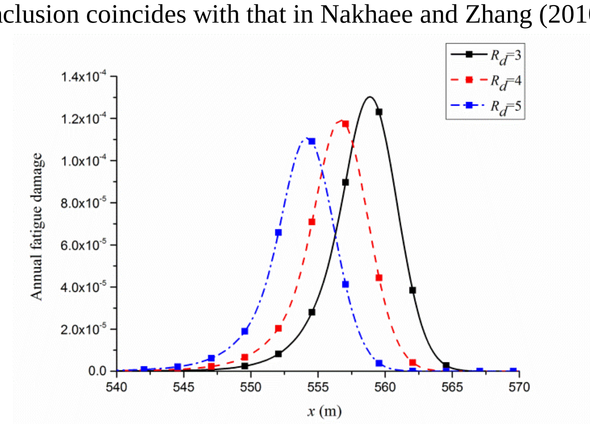

Fig. 7 Annual fatigue damage near TDP with different R_d

EFFECT OF LOW FREQUENCY RESPONSE

Under the ocean environment SCR is subjected to lots of loads, such as wave frequency and low frequency response of floating structure, vortex induced vibration, slug, etc. The effect of the low frequency response on the trench is here discussed since it can drive large displacement of the SCR. Fig. 8 demonstrates the comparison between the surrogate model and numerical trench induced by wave frequency and low frequency responses. The low frequency response amplitudes in Figs. 8(*a*) and 8(*b*) are equal to 10 m and 20 m respectively. The periods are both 100 s. It can be seen that compared with the surrogate model the low frequency may push TEP closer to the hang-off point, thus the fore part of the trench would be less steep. Additionally, the surrogate model seems to more accurately describe the stern part of the trench when the low frequency amplitude is large.

(*a*)

(*b*)

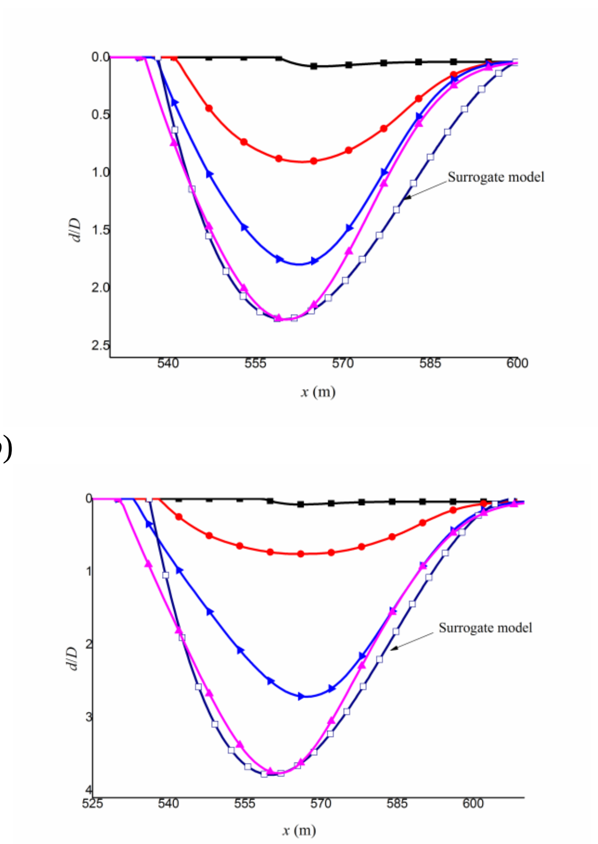

Fig. 8 Comparison of surrogate model with trench induced by low frequency response

CONCLUSIONS

The present study takes the numerical seabed trench obtained from OrcaFlex as benchmark, and compares it with two empirical seabed trench models: cubic polynomial model and quadratic exponential model. The former shows good agreement with the numerical trench. By analyzing the matching conditions between static SCR and numerical trench, a SCR-trench matching criterion is proposed, and then an in-house code is developed based on the interface between OrcaFlex and C++ to find the optimum trench length and position. The sensitivity of the trench length and position to the riser mass per unit length, ratio of horizontal span to vertical span and trench depth is parametrically investigated. This study applies the obtained data to fit the prediction equations of trench length and position, and takes them as surrogate model. Trench length and positon of numerical trenches and related fatigue damage of SCR near TDP are compared with those based on surrogate model. The results show good agreement. Based on the surrogate model the effect of trench development on the fatigue damage near TDP is then studied. The results indicate that trench development may benefit the fatigue lift near TDP.

ACKNOWLEDGMENTS

This work is financially supported by NUS Start-up (Grant No. R-302-000-099-133).

REFERENCES

[1] 2H Offshore Engineering Ltd. STRIDE JIP – Effects of Riser/Seabed Interaction on SCR. 2002, Report No. 1500-RPT-008.

[2] Aubeny C.P., Biscontin G. Interaction Model for Steel Compliant Riser on Soft Seabed. Offshore Technology Conference, 2008, Houston, Texas, USA.

[3] Aubeny C.P., Biscontin G. Seafloor-Riser Interaction Model. International Journal of Geomechanics, 2009, Vol. 9, pp: 133-141.

[4] Nakhaee A., Zhang J. Trenching effects on dynamic behavior of a steel catenary riser. Ocean Engineering, 2010, Vol. 37, pp: 277-288.

[5] Bai X.L., Huang W.P. and Vaz M.A. Riser-soil interaction model effects on the dynamic behavior of a steel catenary riser. Marine Structures, 2015, Vol. 41, pp: 53-76.

[6] Orcina Ltd. OrcaFlex Manual, Version 9.7c. 2014.

[7] Randolph M., Quiggin P. NON-LINEAR HYSTERETIC SEABED MODEL FOR CATENARY PIPELINE CONTACT. Proceedings of the ASME 2009 28th International Conference on Ocean, Offshore and Arctic Engineering, 2009, Honolulu, Hawaii, USA.

[8] Shiri H. Response of steel catenary risers on hysteretic non-linear seabed. Applied Ocean Research, 2014a, Vol. 44, pp:20-28.

[9] Elosta H., Huang S. and Incecik A. Dynamic response of steel catenary riser using a seabed interaction under random loads. Ocean Engineering, 2013, Vol. 69, pp: 34-43.

[10] Elosta H., Huang S. and Incecik A. Trenching effects on structural safety assessment of integrated riser/semisubmersible in cohesive soil. Engineering Structures, 2014, Vol. 77, pp: 57-64.

[13] Thethi R., Moros T. Soil interaction effects on simple catenary riser response. Deepwater Pipeline & Riser Technology Conference, 2001, Houston, Texas, USA.

[14] Bridge C.P., Howells H.A. Full scale model tests of a steel catenary riser. Report, 2003, 2H Offshore Engineering Ltd.

[15] Li F.Z., Low Y.M. Fatigue reliability analysis of a steel catenary riser at touchdown point incorporating soil model uncertainties. Applied Ocean Research, 2012, Vol. 38, pp: 100-110.

[16] Shiri H. Influence of seabed trench formation on fatigue performance of steel catenary risers in touchdown zone. Marine Structures, 2014b, Vol.36, pp:1-20.

[17] Wang K.P., Low Y.M. A simple parametric formulation for the seabed trench profile beneath a steel catenary riser. Marine Structures, 2016, Vol45, pp:22-42.

[18] DNV. RISER FATIGUE. 2005, Norway.

[19] Bridge C., Howells H. Observations and Modeling of Steel Catenary Riser Trenches. Proceedings of the Seventeenth International Offshore and Polar Engineering Conference, 2007, Lisbon, Portugal.

Table 1 Parameters of nonlinear pipe-soil interaction model

Parameter	Symbol	Value
Mudline shear strength	S_{u0}	1.5 kPa
Shear strength gradient	ρ	2.5kPa/m
Power law parameter	a	6.5
Power law parameter	b	0.25
Normalized maximum stiffness	K_{max}	200
Suction ratio	f_{suc}	0.6
Suction decay parameter	λ_{suc}	0.5
Repenetration parameter	λ_{rep}	0.4

Table 2 Values of normalized parameters

Normalized parameters	Values
R_d	1.5, 2.0, 2.5, 3.0, 3.5, 4.0, 4.5, 5.0
R_M	1.4, 1.6, 1.8, 2.0, 2.2, 2.4, 2.6 ,2.8, 3.0
R_{HV}	0.361, 0.456, 0.560, 0.675, 0.803, 0.954, 1.129

Table 3 Comparison of numerical trench results with surrogate model

(R_M, R_{HV})	R_d	R_L		R_{TP}	
		Numerical results	Surrogate model	Numerical results	Surrogate model
(2.2, 0.56)	2.60	228.8	218.8	–86.2	–89.8
	4.30	280.4	275.7	–104.5	–107.1
(2.2, 0.803)	1.75	221.5	228.5	–87.5	–90.7
	3.40	311.3	312.0	–113.3	–116.2